High-Efficiency focusing grating coupler with distributed Bragg reflector

WEI JINMEI,[1] LI YAN,[1*] ZHANG YUEJUN,[1*] LI XIANG YU[1] ,DAI TINGGE[2] AND ZHANG XIAOWEI[1]

[1] *Faculty of Electrical Engineering and Computer Science, Ningbo University, Ningbo 315211, China*

[2] *Ningbo Innovation Center, Zhejiang University, Ningbo 315100 China*

*zhangyuejun@nbu.edu.cn; *liyan4@nbu.edu.cn.

Abstract: We propose a high-efficiency silicon nitride focusing grating coupler with a bottom reflector. The bottom reflector consists of a distributed Bragg reflector (DBR) with a stack of Si_3N_4 and SiO_2 layers. Moreover, the taperless structure of focusing grating couplers is utilized to further increase the density of integration. The result shows that the reflectivity of the grating coupler with 8-layer DBR reaches 98% at 1550nm, the peak coupling efficiency (CE) is −2.1dB and the 1dB bandwidth is 66nm. Compared to the focusing grating without DBR, the CE is improved by 1.87 dB with slight change in 1dB bandwidth, and the footprint is only $27.1\times 37.1\mu m^2$.

1. Introduction

Loss reduction is one of the most essential and emergent issues that should be tackled in photonic integrated circuits (PICs). Due to its low-loss property and transparency across a broad wavelength range (400-2350nm), silicon nitride (Si_3N_4) has been considered as a promising platform[1-5]. It has been widely used in communication[6], sensing[7], computation[8] and quantum physics[9].

Lots of optical coupling methods have been already utilized, however, the low-loss optical coupling is still a serious challenge in Si_3N_4 platform. The grating coupler (GC) is one of the most commonly used coupling methods to achieve flexible wafer-scale testing[10-11]. The coupling efficiency (CE) of grating couplers is mainly related to directionality and mode mismatch. The Si_3N_4 GC has been proposed and fabricated in ref.[12], but the coupling efficiency is only 27%, which is caused by the fact that most of the optical power is dissipated downward into the substrate, resulting in poor directionality. To solve this problem, several approaches have been proposed. Dual-level or silicon overlay in Si_3N_4 grating coupler has been reported to improve the directionality, but the complexity is significantly increased[13-14]. And the other approach is using bottom reflectors such as metal mirrors or distributed Bragg reflectors (DBR) to cover the light scattered towards the substrate. However, the metal mirror is fragile at high temperatures and the fabrication process of reflectors is relatively complex and incompatible with CMOS fabrication[15-16].

In this paper, a high-efficiency focusing Si_3N_4 grating coupler is proposed. In order to improve the directionality, a DBR consisting of a stack of silicon nitride and silicon dioxide is employed as the bottom reflector. The reflectivity can reach 98% with 8-layer DBR at a wavelength of 1550nm. Furthermore, a focusing grating instead of a linear grating is utilized to reduce the footprint, therefore, improve the integration density.

2. Simulation and design

The schematic of the proposed Si_3N_4 GC is shown in Fig. 1(a). In order to reduce P_{down} and enhance directionality, a stack of the multilayer DBR is deposited on the Si substrate, and a 400 nm fully etched Si_3N_4 layer is deposited on the buried oxide (BOX) layer, a SiO_2 cladding layer covers the Si_3N_4 GC to protect the device.

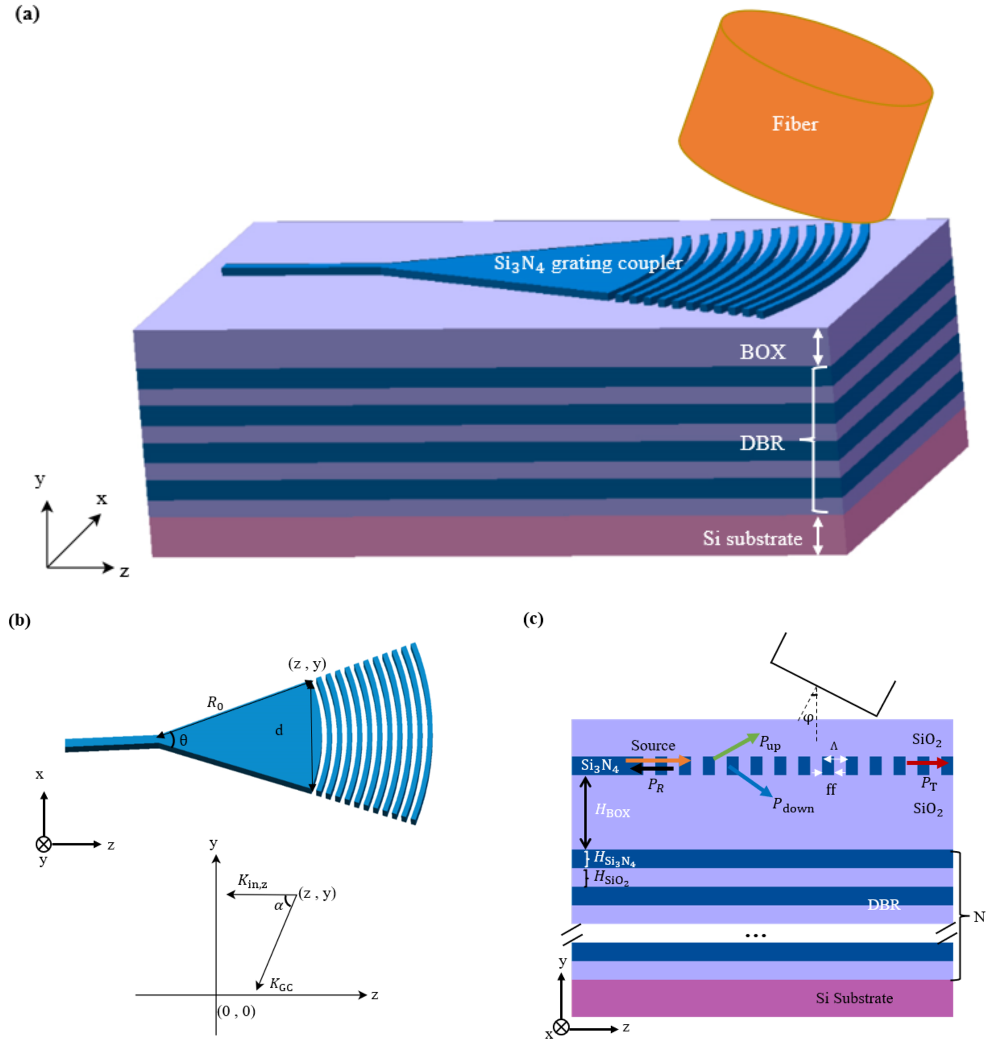

Fig. 1. (a) 3D schematic of the grating coupler with multiple layers DBR; (b) Structure diagram of the focusing grating coupler and wave vector at (*z*, *y*); (c) Cross-sectional view of a grating coupler with DBR and the distribution of power when light is coupled into the grating.

2.1 Gratings on 400 nm Si_3N_4

Fig. 1(b) shows the structure diagram of the focusing grating coupler and the wave vector of the fan-shaped grating coupler at (*z*, *y*). In order to achieve the phase of constructive interference, the following requirements should be met:

$$K_{\mathrm{in,z}} \cos \alpha r + 2\pi m = K_{\mathrm{GC}} r \qquad (2\text{-}1)$$

where K_{GC} is the wave vector of the waveguide, α is the angle between the connection vector of (*z*, *y*) and the center of the circle (0, 0) and the *z*-axis, $r = \sqrt{z^2 + y^2}$ is the distance from (*z*, *y*) to (0, 0), *m* is an integer number, $K_{\mathrm{in,z}} = (2\pi n_{\mathrm{c}} \cdot sin\varphi)/\lambda$ is the projected component of the incident wave vector in the grating plane, n_c is the refractive index of cladding material, λ is the center wavelength, $K_{GC} = (2\pi n_{eff})$ is the wave vector size of the grating waveguide, n_{eff} is the effective index of the grating. To satisfy the Bragg condition at first order:

$$n_{eff} - n_c \cdot \sin\varphi = \frac{\lambda}{\Lambda} \tag{2-2}$$

where Λ is the period of grating coupler, φ is the coupling angle, n_{eff} is calculate as:

$$n_{eff} = ff \cdot n_{eff1} + (1 - ff) \cdot n_{eff2} \tag{2-3}$$

where ff is the filling factor defined as the ratio of grating teeth to the period, n_{eff1} is the refractive index of the grating teeth and n_{eff2} is the refractive index of the etched region.

The finite-difference time-domain (FDTD) has been used to optimize GC structures. Fig. 1(c) shows various power distribution, P_{up}/P_{down} represent the upward/downward power and P_T/P_R is the transmit/reflect power. Fig. 2(a) shows coupling efficiency as a function of the filling factor. The fill factor affects the performance of a grating coupler by changing the effective index, via Equation (2-2). Hence, as the fill factor increases, the effective index increases. The result shows that ff=0.5 is optimal. The spectra of grating couplers with different periods (Λ) are shown in Fig. 2(b). The grating period is the parameter with the most impact on the grating wavelength, as seen by Equation (2-2). As the grating period varied from 1.03μm to 1.05μm, the central wavelength of the grating coupler shifted from 1537nm to 1558nm. The wavelength has a red shift as the period increases. According to Eq.(2-2), the coupling efficiency is related to coupling angle (φ). When ff=0.5 and Λ=1.04μm, CE with different φ is shown in Fig. 2(c). The wavelength has a blue shift as coupling angle increases. Therefore, φ=11° is chosen to achieve the maximum coupling efficiency of −3.97dB at $\lambda = 1550$nm.

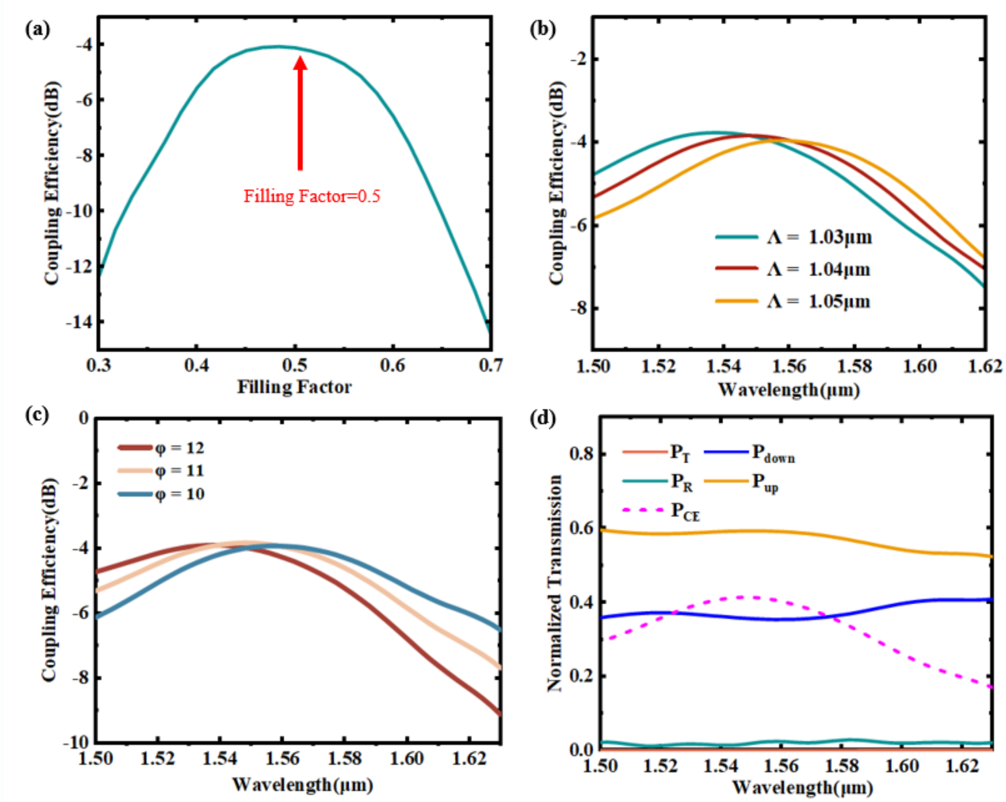

Fig. 2. (a) The coupling efficiency as a function of the filling factor; (b) The coupling efficiency as a function of the period of GC; (c) The coupling efficiency as a function of coupling angle; (d) The optimized power distribution of various transmission directions with the period of 1.04μm and fill factor of 0.5.

Fig. 2(d) shows the spectral response with a period of 1.04μm and a fill factor of 0.5. Although the grating period and the filling factor have been optimized, the substrate leakage P_{down} accounts for a substantial portion of the total scattered power loss. In order to reduce P_{down} and enhance directionality, the bottom reflector using multiple DBR stacks is proposed.

2.2 Design of DBR

Each layer of DBR consists of a high-index material Si_3N_4 and a low-index material SiO_2, the thickness of Si_3N_4 and SiO_2 are calculated according to $\lambda/4n$ [18] (λ is the center wavelength of the source and n is the refractive index of materials), so after calculation the thickness of Si_3N_4 and SiO_2 was set as 194 nm and 268 nm, respectively.

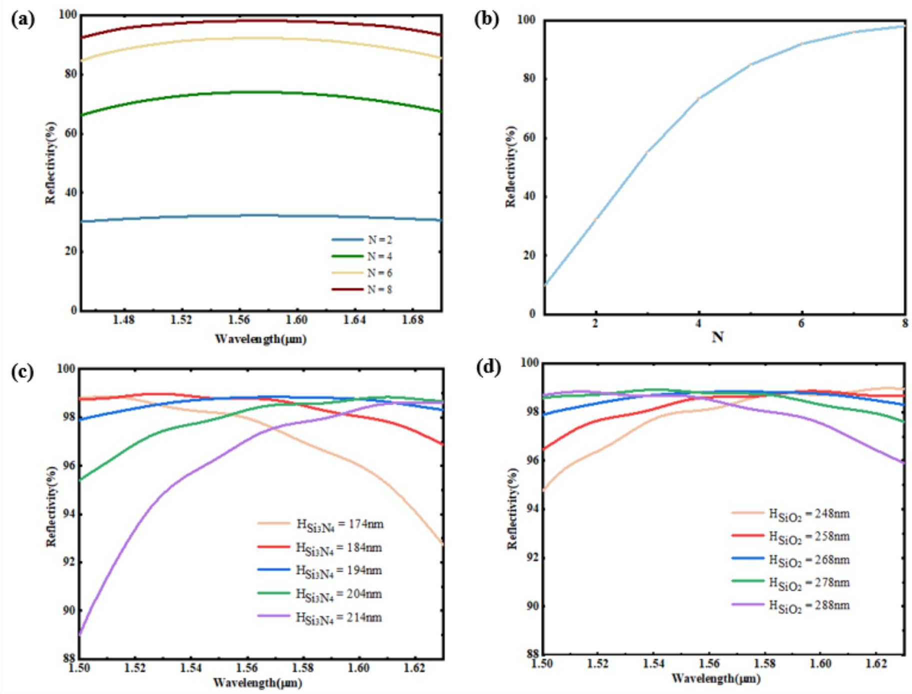

Fig. 3 (a) Reflectivity as a function of the wavelength when the DBR reflection layer is 2, 4, 6, and 8, respectively; (b) Reflectivity as a function of the layers when wavelength at 1550nm; (c) Reflectivity with SiO_2 film thickness variation when Si_3N_4 thickness is 194 nm; (d) Reflectivity with Si_3N_4 film thickness variation when SiO_2 thickness is 268 nm, while the thickness variation scanning step is 10nm.

Fig. 3(a) shows the reflectivity as a function of wavelength with the different numbers of layers N of DBR. As shown in Fig. 3(b), as the increase of N, the reflectivity increases slowly. When N=8, the reflectivity almost can keep at a constant 96.7% for wavelength ranging from 1400nm to 1600nm. As shown in Fig. 3(c) (d), the reflectivity spectrum varies slightly with the thickness of SiO_2 film and Si_3N_4 film, respectively, i.e., large fabrication tolerance.

2.3 Design of BOX

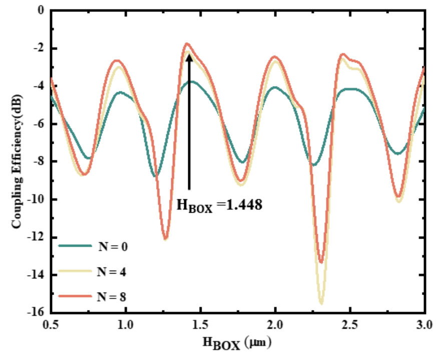

Fig. 4. Coupling efficiency as a function of BOX thickness.

BOX layer is utilized to prevent mode leakage, and a specific BOX thickness can achieve constructive interference between the reflected light and the directly upward radiated light, thereby reducing the loss. Therefore, the thickness of the BOX layer between the grating and the reflector needs to be calculated and optimized. Fig. 4 shows that the coupling efficiency is highly dependent on the BOX thickness(H_{box}). Form calculation, H_{box}=1.448μm is set to achieve the constructive interference.

2.4 Impact of DBR Stacks

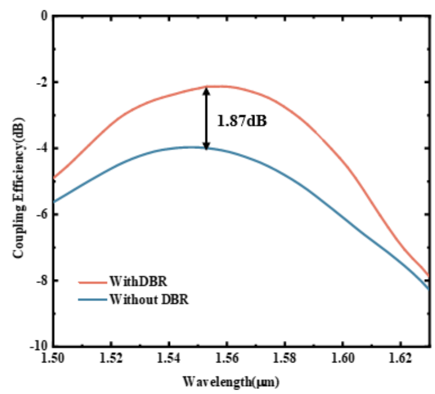

Fig. 5. Comparison of coupling spectrum between without and with the DBR stacks.

Fig. 5 shows the comparison of the coupling spectrum without and with the DBR stack, which are −3.97dB and −2.1dB, and the 1dB bandwidth reaches 66nm, which is much larger than that of the Sillion grating coupler. Moreover, the influence of DBR on the bandwidth can be neglected. From the comparison, table 1, our proposed focusing grating shows quite great performance.

Table 1. Comparison of the performance of different SiN grating couplers

Ref.	Bottom reflector	Gratings	Max CE (dB)	1dB Bandwidth(nm)	t_{SiN} (nm)	Footprint (μm)
[17]	Si-SiO_2	linear grating	−2.5	53	400	13×530
[18]	α-Si-SiO_2	linear grating	−2.29	49	500	12×\

[18]	α-Si-SiO_2	linear grating	−2.58	52	400	12×\
[16]	SiNx-SiO_2	linear grating	−2.4	52.5	325	13×530
[19]	AlCu/TiN	focusing gratings	−2.29	\	100	28×100
This work	Si_3N_4-SiO_2	focusing gratings	−2.1	66	400	27.1×37.1

3. Conclusion

In conclusion, a high-efficiency focusing Si_3N_4 grating coupler with DBR is demonstrated. The directionality of GC is optimized by adding DBR consisting of a stack of silicon nitride and silicon dioxide as the bottom reflector, and the fan-shape focusing grating is used to improve the density of integration. The result shows that the reflectivity reaches 98% at a wavelength of 1550nm. The peak coupling efficiency is −2.1dB the bandwidth is 66nm, and the footprint is only 27.1×37.1μm^2. The performance of the grating coupler can be further improved by optimizing its filling factor.

Acknowledgment

This work was supported by the National Natural Science Foundation of China (62205164, 62005242, 62134002, 61974078), Natural Science Foundation of Zhejiang (LQ20F050001), National Key Research and Development Program of China (2021YFB2800201), Natural Science Foundation of Ningbo (2021S066).

References

1. P. J. Winzer, D. T. Neilson, A. R. Chraplyvy, "Fiber-optic transmission and networking: the previous 20 and the next 20 years." *Optics Express*. **26**(18), 24190-24239 (2018).
2. R. Baets, A. Z. Subramanian, S. Clemmen, B. Kuyken, P. Bienstman, N. L. Thomas, G. Roelkens, D. V. Thourhout, P. Helin, S. Severi, "Silicon Photonics: silicon nitride versus silicon-on-insulator," *Optical Fiber Communication Conference. Optical Society of America*, (2016).
3. C. Xiang, W. Jin, J. E. Bowers, "Silicon nitride passive and active photonic integrated circuits: Trends and prospects," *Photonics Res*. **10**, A82–A96 (2022).
4. F. Gardes, A. Shooa, P. G. De, I. Skandalos, S. Ilie, T. Rutirawut, W. Talataisong, J. Faneca, V. Vltali, Y. Hou, T. Bucio, L. Zeimpekis, C. Lacava, P. Petropoulos, "A review of capabilities and scope for hybrid integration offered by silicon-nitride-based photonic integrated circuits," *Sensors*, **22**, 4227 (2022).
5. M. Borghi, C. Castellan, S. Signorini, A. Trenti, L. Pavesi, "Nonlinear silicon photonics," *Journal of Optics*. **19**(9), 093002 (2017).
6. C. Doerr, "Silicon photonic integration in telecommunications," *Frontiers Phys*, **3**(37), (2015).
7. K. De Vos, I. Bartolozzi, E. Schacht, P. Bienstman, R. Baets, "Silicon-on-insulator microring resonator for sensitive and label-free biosensing," *Opt. Express*, **15**(12), 7610-7615 (2007).
8. B. J. Shastri, A. N. Tait, T. Ferreira de Lima, W. H. Pernice, H. Bhaskaran, C. D. Wright, P. R. Prucnal, "Photonics for artificial intelligence and neuromorphic computing," *Nature Photonics*,**15**(2),102-114 (2021).
9. J Wang, F Sciarrino, A Laing, M. G. Thompson, "Integrated photonic quantum technologies," *Nature Photonics*, **14**(5), 273-284 (2020).
10. G. Son, S. Han, J. Park, K. Kwon, K. Yu, "High-efficiency broadband light coupling between optical fibers and photonic integrated circuits," *Nanophotonics*, **7**(12), 1845-1864 (2018).
11. L. Cheng, S. Mao, Z. Li, Y. Han, H. Y. Fu, "Grating couplers on silicon photonics: Design principles, emerging trends, and practical issues," *Micromachines*, **11**(7), 666 (2020).
12. C. R. Doerr, L. Chen, Y.-K. Chen, and L. L. Buhl, "Wide bandwidth silicon nitride grating coupler," *IEEE Photonics Technol. Lett.* **22**(19), 1461–1463 (2010).
13. V. Vitali, C. Lacava, T. Domínguez Bucio, F. Y. Gardes, P. Petropoulos, "Highly efficient dual-level grating couplers for silicon nitride photonics," *Scientific Reports*, **12**(1): 1-12 (2022).
14. B. Chmielak, S. Suckow, J. Parra, V. C. Duarte, T. Mengual, M. A. Piqueras, A. L. Giesecke, M. C. Lemme, P. Sanchis, "High-efficiency grating coupler for an ultralow-loss Si_3N_4-based platform," *Optics Letters*, **47**(10),2498-2501 (2022).

15. W. S. Zaoui, M. F. Rosa, W. Vogel, M. Berroth, J. Butschke, F. Letzkus, "Cost-effective CMOS-compatible grating couplers with backside metal mirror and 69% coupling efficiency," *Optics Express*, **20**(26), B238-B243 (2012).
16. J. Hong, A. M. Spring, F. Qiu, ShiyoshiYokoyama, "A high efficiency silicon nitride waveguide grating coupler with a multilayer bottom reflector," *Scientific reports*, **9**(1), 1-8 (2019).
17. H. Zhang, C. Li, X. Tu, J. Song, H. Zhou, X. Luo, Y. Huang, M. Yu, G. Q. Lo, "Efficient silicon nitride grating coupler with distributed Bragg reflectors," *Optics Express*, **22**(18), 21800-21805 (2014).
18. S. Nambiar, A. Kumar, R. Kallega, P.Ranganath, S. K. Selvaraja, "High-efficiency grating coupler in 400 nm and 500 nm PECVD silicon nitride with bottom reflector," *IEEE Photonics Journal*, **11**(5), 1-13 (2019).
19. S. Romero-García, F. Merget, F. Zhong, H. Finkelstein, J. Witzens, "Visible wavelength silicon nitride focusing grating coupler with AlCu/TiN reflector," *Optics Letters*, **38**(14), 2521-2523 (2013).